Spectrum of Engineering Sciences
ISSN (e) 3007-3138 (p) 3007-312X Volume 4, Issue 3, 2026

NUMERICAL MODELLING AND SIMULATION OF LEAD-FREE CHALCOGENIDE PEROVSKITES BY USING 1-D SOLAR CELL CAPACITANCE SIMULATOR

Azmat Ali[*1], Ahmed Salim[2], Mohsin M. Tarar[3]

[*1]Department of Physics, University of Chakwal, Chakwal, Pakistan
[2]Department of Electrical Engineering, NAMAL University Mianwali, Pakistan
[3]Department of Electronics Engineering, University of Chakwal, Chakwal, Pakistan

[*1]azmat.chakwal@gmail.com, [2]ahmed.salim@namal.edu.pk, [3]mohsin.tarar@uoc.edu.pk

DOI: https://doi.org/10.5281/zenodo.22053939

Keywords
Chalcogenide Perovskites, Solar Energy, lead Free, SCAPS-1D, Numerical Simulations

Article History
Received: 27 January 2026
Accepted: 12 March 2026
Published: 26 March 2026

Corresponding Author: *
Azmat Ali

Abstract

In this study we investigates the potential use of chalcogenide perovskites absorbers ($BaHfS_3$ and $SrHfS_3$), for solar cell applications. The electrical and optical properties of these absorbers are examined in a simulated solar cell structure consisting of SnS_2 as the electron transport layer and Sb_2S_3 as the hole transport layer. The Solar Cell Capacitance Simulator (SCAPS-1D) was used to conduct these simulations. Bandgap energies, electron affinities, dielectric constants, mobilities, and defect concentrations are important considerations in optimizing layer thicknesses and interface properties. The study will evaluate solar cell performance indicators such as fill factor, open-circuit voltage, power conversion efficiency, and current density. The results demonstrate that, $BaHfS_3$ generates carriers more efficiently and maintains a higher current density than $SrHfS_3$ in solar cell. Both materials show excellent quantum efficiency in the visible spectrum; however, $BaHfS_3$ has a little edge over $SrHfS_3$.

Introduction

The name "perovskite" was in the honor of renowned scientist Count Lev Alekseevich von Perovski. Gustav Rose who discovered the first perovskite, $CaTiO_3$, in 1839 [1-3]. Perovskite materials are superconducting metallic, insulating, and semiconducting in nature[4]. They are used for filtering, photochromic, optical switching, electro chromic, and surface acoustic wave signal processing [5]. The discovery and investigation of perovskite materials has changed the photovoltaic (PV) industry in the recent decades. This term refers to hybrid organic/inorganic halides which have crystallized into structures. These materials consist of an organic cation (A), a metal cation (B), and a halide anion (X) which are referred to as ABX_3[6, 7] [7]. They have proven to be remarkably effective at absorbing light from solar cells [8, 9] [9] [10-12] [12]. However, concerns have been expressed due to their long-term stability[13] and toxicity [14]. To overcome these limitations, researchers are in search of their alternative materials[15]. Chalcogenide perovskites' favorable properties, make them as a potentially effective option [16, 17] [17] [18] [19] [20]. SpectrumChalcogenide perovskites, contains chalcogen elements e.g tellurium, selenium, or sulfur, having tunable high absorption coefficients, bandgaps, and carrier mobilities as comparable to halide perovskites, making them suitable for optoelectronic devices such as LEDs, solar cells, and photodetectors [20]. Chalcogenide perovskites are more ecologically benign and chemically stable than their halide perovskites, making them more favorable for commercial use. As a result, they have piqued the interest of many scholars in recent years [21, 22] [22].

The crystal structure of chalcogenide perovskites is similar to that of normal perovskites. They are suitable for successful solar cells which can capture a majority portion of the light spectrum due to their tunable visible/UV bandgaps,

which allow them to absorb a range of wavelengths [23]. These materials are preferable over oxide and halide perovskites[7] due to their high temperature stability, lower toxicity, and resistance to aquatic environments[24, 25] [25]. Researchers are actively working on development of nano-scale materials with interesting optical properties in order to manufacture long lasting, highly effective and cheaply cost optoelectronic devices[26, 27] [27]. The band-gaps of $BaZrS_3$ and $SrHfS_3$ chalcogenid- perovskites, are 1.8-1.9 eV and 2.4-2.5 eV, respectively [28]. In 2018 and 2019, it was reported that $BaHfS_3$, had a bandgap of 2.06 eV at 79.1% purity with a formation energy of -1.756 eV/f.u. $SrHfS_3$, introduced in 1980, is noted for its green photoluminescence and ability to emit green light. With a bandgap of 2.41 eV, it was synthesized in powder form in 2020 while retaining a distorted perovskite phase [29].

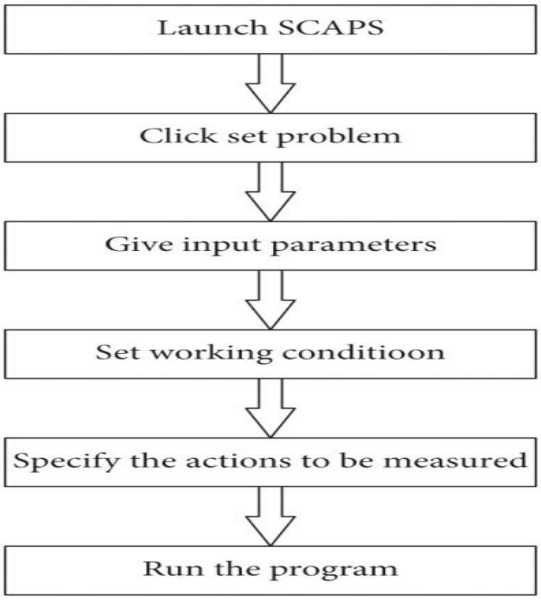

Fig.1 SCAPS-1D simulation process [27].

In this work, SCAPS simulation software was used to perform a multi-physics simulation of $BaHfS_3$ and $SrHfS_3$ perovskites. The simulated device structure was consist of three layers: an electron transport layer (ETL), a hole transport layer (HTL) and absorber layer composed of SnS_2, Sb_2S_3, and $BaHfS_3$ or $SrHfS_3$ respectively. Our aim to investigate the properties and behavior of these materials in a solar cell device.

Methodology

The SCAPS-1D (Solar Cell Capacitance Simulator) version 3.3.08 [30] is used in the optimization and modeling of perovskite solar cell (PSC). This simulator was developed by the University of Gent in, which uses an algorithm based on three correlated partial differential equations (PDEs): Poisson's equation, the continuity equations for electrons and the electron continuity equation. The program's many panels enable users to calculate results and change parameters. Figure 1 depicts the step by step SCAPS program's simulation approach.

In this article, the SCAPS-1D was used investigate the performance of perovskite solar cells (PSCs) with active absorber materials $SrHfS_3$ and $BaHfS_3$ with SnS_2 serving as the electron transport layer (ETL) and Sb_2S_3 as the hole transport layer (HTL). In addition to opto-electrical properties, each material's bandgap, electron affinity, dielectric constant, mobility, and defect concentration were considered. The simulation parameters which includes layer thicknesses, interface defects, standard illumination settings (AM1.5G, 1000 W/m2), and recombination, generations and Shockley-Read-Hall (SRH) recombination are considered.

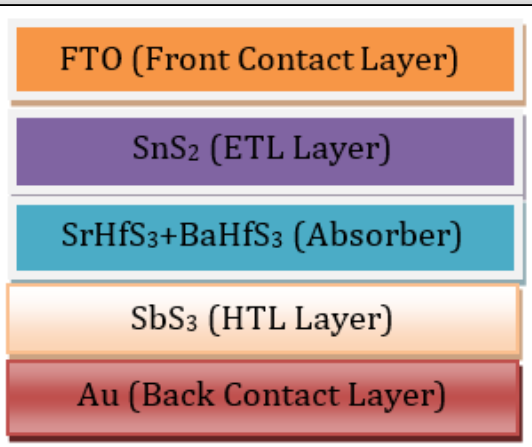

Fig.2 Layered structure of a solar cell with different materials

A range of solar cell parameters at different layer thicknesses and temperatures, including current density (Jsc), fill factor (FF,%), power conversion efficiency (PCE,%), and open-circuit voltage (Voc) are calculated. Furthermore, seven different layers of the solar cell were examined using SCAPS-1D simulations in both dark and light conditions and at various temperatures [31] [32].

Results and Discussion

The figures show the performance of $BaHfS_3$ and $SrHfS_3$ absorbers in solar cells at various thicknesses. Figure (a) shows that $SrHfS_3$ has 19% efficiency, while $BaHfS_3$ reaches 28% efficiency at 1 µm thickness. This shows that $BaHfS_3$ is more suitable for solar cell applications. Figure (b) shows that the fill factor (FF) for both absorbers. Which decreases as thickness increases, starting at 87.5% for $BaHfS_3$ and 88.5% for $SrHfS_3$. This shows the importance of getting ideal Fill Factor FF% and efficiency eta% while balancing thickness. Figure (c) shows that $SrHfS_3$ has a greater short-circuit current density (J_{SC}) as compare to $BaHfS_3$. Finally, figure (d) shows that $BaHfS_3$ has a higher V_{OC} as a function of thicknesses, with an ideal thickness of around 0.5 µm, but $SrHfS_3$ improves V_{OC} up to 2 µm. This demonstrates how crucial it is to select the ideal material and thickness for the optimal functioning of solar cells. The graph illustrates the impact of capacitance on voltage in solar cells made from $SrHfS_3$ and $BaHfS_3$. The capacitance of both materials is nearly consistent across the voltage range of -1 V to 0.5 V. The capacitance of $BaHfS_3$ increases faster as the voltage approaches 1 V, indicating a transition area with potential charge carrier accumulation or nonlinear effects. This means that material choice may affect solar cell performance.

The energy band diagrams for optimized $BaHfS_3$ and $SrHfS_3$ solar cells illustrate the conduction and valence band boundaries as a function of thickness (0–1 µm) and energy

Table 1 Input parameters of ETM, HTM and both absorbers used in this study.

Material parameters	SnS_2	Sb_2S_3	$BaHfS_3$	$SrHfS_3$
Thickness(µm)	0.05	0.2	1.0	1.0
Band gap (eV)	2.2	1.7	1.53	1.96
Electron affinity (eV)	4.24	3.7	4.6	4.0
dielectric permittivity (relative)	9.0	19	7.39	8.41
CB effective density of states (cm^{-3})	2.2×10^{18}	2.2×10^{19}	1.0×10^{19}	1.0×10^{18}
VB effective density of states (cm^{-3})	1.8×10^{19}	5.5×10^{20}	1.0×10^{19}	1.0×10^{19}
electron thermal velocity (cms^{-1})	1.0×10^{7}	1.0×10^{7}	1.0×10^{7}	1.0×10^{7}
hole thermal velocity (cms^{-1})	1.0×10^{7}	1.0×10^{7}	1.0×10^{7}	1.0×10^{7}

electron mobility ($cm^2V^{-1}s^{-1}$)	1.0×10^{2}	1.0×10^{2}	5.0×10^{1}	5.0×10^{1}
hole mobility ($cm^2V^{-1}s^{-1}$)	2.5×10^{1}	1.0×10^{-1}	5.0×10^{1}	5.0×10^{1}
shallow uniform donor density ND (1/cm3)	1.0×10^{18}	0	1.0×10^{15}	1.0×10^{15}
shallow uniform acceptor density NA (1/cm3)	0	1.0×10^{15}	1.0×10^{15}	1.0×10^{15}

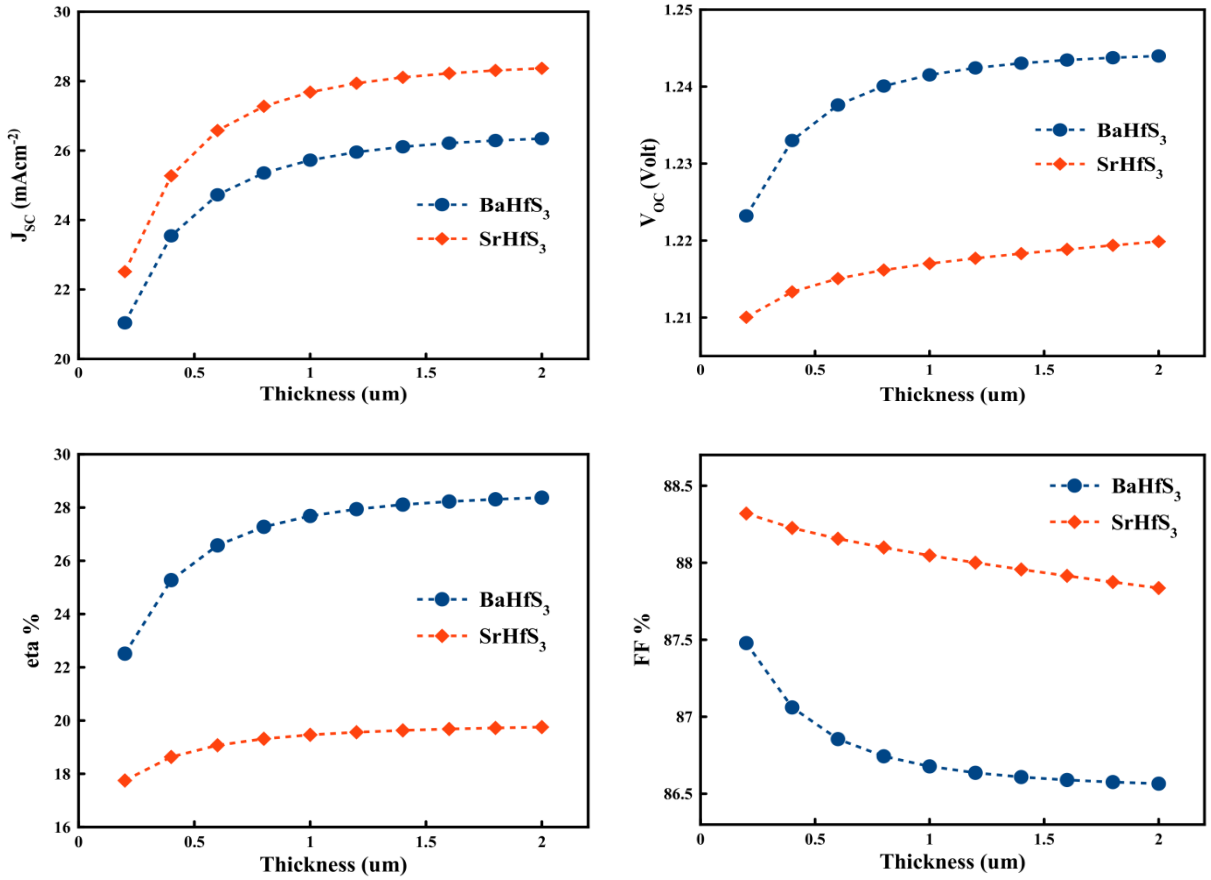

Fig.3 Optimization of thickness of absorber layer in SnS_2 (ETL) + $BaHfS_3$/$SrHfS_3$ + Sb_2S_3 (HTL) solar cell.

levels (-2 eV to 2 eV). Both materials' staggered energy band topologies include multiple steps, indicating that the composition changes at different thicknesses. The valence band (E_V) and conduction band (E_C) must align for effective charge separation and transport. $BaHfS_3$ shows significant band edge variations with thickness, indicating successful charge separation, but $SrHfS_3$ has a distinct profile. These factors influence the optical and electrical properties; increasing thickness can boost efficiency by improving charge carrier separation and minimizing recombination losses.

The graph shows that both $SrHfS_3$ and $BaHfS_3$ generate carriers over 0.5V, with $BaHfS_3$ having a higher generation efficiency of 5.8 x 10^{-4}. $BaHfS_3$ may be more effective for solar cell applications because higher carrier generation leads to higher conversion efficiency.

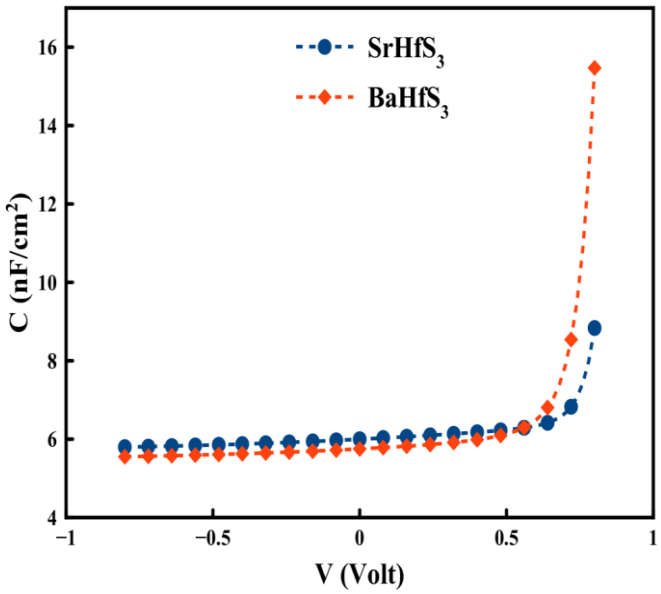

Fig.4 Capacitance of Voltage of optimized solar cell

This is significant because it has an immediate impact on the solar cells' ability to convert incident light into electrical power. Thus, $SrHfS_3$ and $BaHfS_3$ may be effective in enhancing solar energy harvesting systems and supporting more environmentally acceptable solar energy solutions.

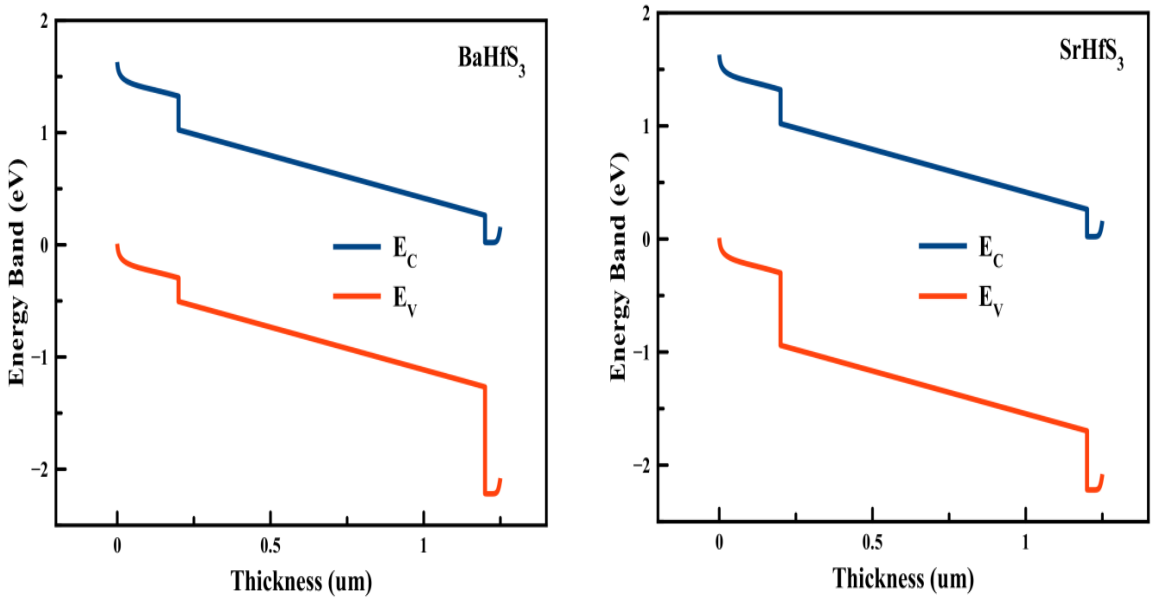

Fig.5 Energy Band diagram of optimized solar cell

The graph illustrates the relationship between total current density and solar cell performance. $SrHfS_3$ and $BaHfS_3$ show a drop in current density as the voltage approaches 1 V, but otherwise remain stable. $BaHfS_3$ has a higher current density, leading to improved electricity generation. Although adjusting thickness can improve efficiency, other factors such as cost and availability must also be considered.

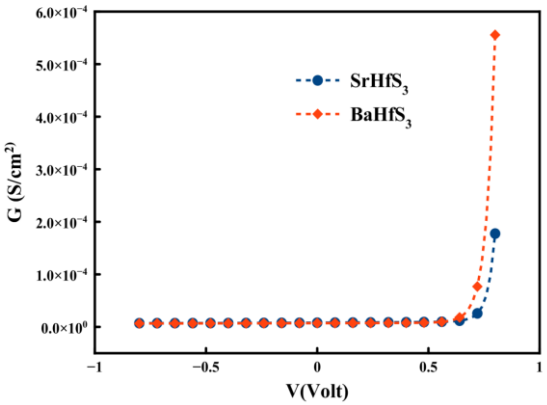

Fig.6 Carrier generation vs. Voltage of optimized solar cell

The graph shows the quantum efficiency (QE) vs wavelength of solar cells optimized with $BaHfS_3$ and $SrHfS_3$ materials. In the visible range (400-700 nm), both materials exhibit significant QE, with $BaHfS_3$ marginally outperforming $SrHfS_3$ in the middle. Beyond 700 nm, QE rapidly decreases, particularly in the near infrared range. Improving the efficiency of these materials in the visible spectrum is crucial to boosting solar energy collection. In multijunction solar cells, using materials with high QE across complementary ranges can improve total efficiency.

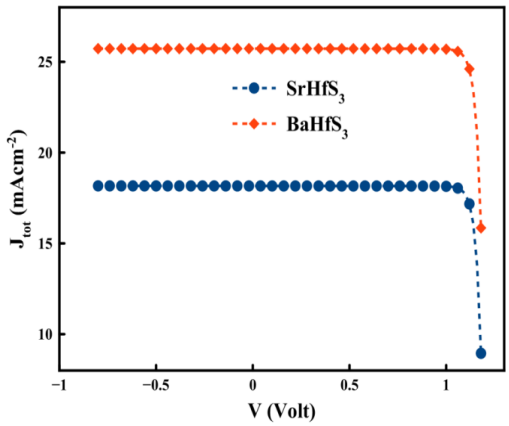

Fig.7 Total current density vs. voltage of optimized solar cell

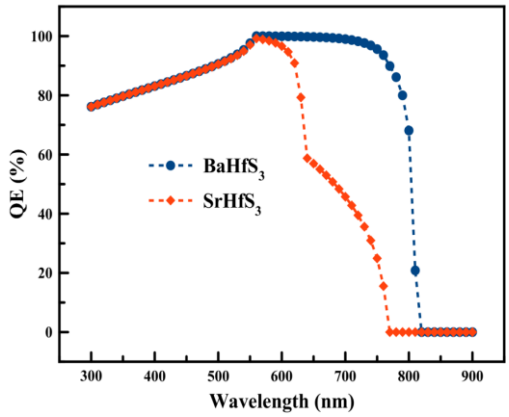

Fig.8 Quantum efficiency vs. Wavelength of Optimized solar cell

Conclusion

The research article investigates the potential of $SrHfS_3$ and $BaHfS_3$ perovskites for use in solar cells through numerical modelling and simulation. The study reveals that $BaHfS_3$ generates carriers more efficiently and maintains higher current density compared to $SrHfS_3$, suggesting its superior performance in photovoltaic applications. The optimization of absorber layer thickness and the material's bandgap alignment are critical for enhancing solar cell efficiency. Calculated electrical parameter shows that $BaHfS_3$ and $SrHfS_3$ has 28% and 19% efficiency with 88.5% and 87.7% fill factor. Both materials exhibit high quantum efficiency in the visible spectrum, with $BaHfS_3$ outperforming $SrHfS_3$. The findings highlight the importance of selecting appropriate materials and optimizing structural parameters to improve solar cell performance, contributing to the development of more efficient and sustainable solar energy solutions.

References

Wolfram, T. and S. Ellialtioglu, *Electronic and optical properties of d-band perovskites*. 2006: Cambridge University Press.

Galasso, F.S., *Structure, properties and preparation of perovskite-type compounds: international series of monographs in solid state physics*. Vol. 5. 2013: Elsevier.

Ali, S., *Synthesis of Nano-particles Using Microwave Technique, the Study of their Physical Properties and Some Applications [PhD thesis]*. Faculty of Science Cairo University, 2009.

Beepat, K., et al., *Perovskite materials for photovoltaics: a review*. The European Physical Journal Applied Physics, 2023. **98**: p. 43.

Ishihara, T., *Perovskite oxide for solid oxide fuel cells*. 2009: Springer Science & Business Media.

Er-raji, O., et al., *Tailoring perovskite crystallization and interfacial passivation in efficient, fully textured perovskite silicon tandem solar cells*. Joule, 2024.

Zhang, N., et al., *Tuning the photoelectric properties of perovskite materials using Mg/Ge/Si and Br double-doped to FASnI3*. The Journal of Physical Chemistry C, 2023. **127**(5): p. 2215-2222.

Jeon, N.J., et al., *Compositional engineering of perovskite materials for high-performance solar cells*. Nature, 2015. **517**(7535): p. 476-480.

Liu, M., M.B. Johnston, and H.J. Snaith, *Efficient planar heterojunction perovskite solar cells by vapour deposition*. Nature, 2013. **501**(7467): p. 395-398.

Xing, G., et al., *Long-range balanced electron-and hole-transport lengths in organic-inorganic CH3NH3PbI3*. Science, 2013. **342**(6156): p. 344-347.

Li, J., et al., *50-Fold EQE improvement up to 6.27% of solution-processed all-inorganic perovskite CsPbBr3 QLEDs via surface ligand density control*. Advanced materials, 2017. **29**(5): p. 1603885.

Zhu, H., et al., *Z. gong, Q. Ding, MV gustafsson, MT Trinh, S. JinandX. Y. Zhu*. Nat. Mater, 2015. **14**: p. 636.

Zhang, H., et al., *Tailoring passivators for highly efficient and stable perovskite solar cells*. Nature Reviews Chemistry, 2023. **7**(9): p. 632-652.

Berry, J., et al., *Hybrid organic–inorganic perovskites (HOIPs): opportunities and challenges*. Advanced Materials, 2015. **27**(35): p. 5102-5112.

Bati, A.S., et al., *Next-generation applications for integrated perovskite solar cells*. Communications Materials, 2023. **4**(1): p. 2.

Sun, Y.-Y., et al., *Chalcogenide perovskites for photovoltaics*. Nano letters, 2015. **15**(1): p. 581-585.

Ye, K., et al., *A Processing Route to Chalcogenide Perovskites Alloys with Tunable Band Gap via Anion Exchange*. Advanced Functional Materials, 2024: p. 2405135.

Surendran, M., et al., *Epitaxial thin films of a chalcogenide perovskite*. Chemistry of Materials, 2021. **33**(18): p. 7457-7464.

Gupta, T., et al., *An environmentally stable and lead-free chalcogenide perovskite*. Advanced Functional Materials, 2020. **30**(23): p. 2001387.

Comparotto, C., et al., *Chalcogenide perovskite BaZrS3: thin film growth by sputtering and rapid thermal processing.* ACS Applied Energy Materials, 2020. **3**(3): p. 2762-2770.

control within chalcogenide perovskites for optimized photovoltaic application. Chemistry of Materials, 2016. **28**(3): p. 821-829.

Wei, X., et al., *Realization of BaZrS3 chalcogenide perovskite thin films for optoelectronics.* Nano Energy, 2020. **68**: p. 104317.

Márquez, J.A., et al., *BaZrS3 chalcogenide perovskite thin films by H2S sulfurization of oxide precursors.* The journal of physical chemistry letters, 2021. **12**(8): p. 2148-2153.

Nie, R., et al., *Halide-chalcogenide hetero-structure for efficient and stable perovskite solar cells.* Chemical Engineering Journal, 2023. **462**: p. 142214.

Han, Y., X. Fang, and Z. Shi, *Advances in chalcogenide perovskites: Fundamentals and applications.* Applied Physics Reviews, 2024. **11**(2).

Yu, Z., et al., *Chalcogenide perovskite BaZrS3 thin-film electronic and optoelectronic devices by low temperature processing.* Nano Energy, 2021. **85**: p. 105959.

Wang, C., et al., *Enhancing the inherent stability of perovskite solar cells through chalcogenide-halide combinations.* Energy & Environmental Science, 2024. **17**(4): p. 1368-1386.

Hanzawa, K., et al., *Material design of green-light-emitting semiconductors: perovskite-type sulfide SrHfS3.* Journal of the American Chemical Society, 2019. **141**(13): p. 5343-5349.

Sopiha, K.V., et al., *Chalcogenide perovskites: tantalizing prospects, challenging materials.* Advanced Optical Materials, 2022. **10**(3): p. 2101704.

Rai, S., B. Pandey, and D. Dwivedi, *Modeling of highly efficient and low cost CH3NH3Pb (I1-xClx) 3 based perovskite solar cell by numerical simulation.* Optical Materials, 2020. **100**: p. 109631.

Huang, L., et al., *Electron transport layer-free planar perovskite solar cells: further performance enhancement perspective from device simulation.* Solar Energy Materials and Solar Cells, 2016. **157**: p. 1038-1047.

Anwar, F., et al., *Effect of different HTM layers and electrical parameters on ZnO nanorod-based lead-free perovskite solar cell for high-efficiency performance.* International Journal of Photoenergy, 2017. **2017**(1): p. 9846310.